Back-to-back aperture- and gap-coupled discontinuities integration for band-pass filter design

A. Nosrati, M. Mohammad-Taheri✉ and M. Nosrati

A new class of back-to-back integrated aperture- and gap-coupled discontinuities is proposed for substrate-integrated waveguide band-pass filter design. The developed structure is shown to take advantage of both discontinuities in the design of cavity and/or planar resonators with an optimum performance including higher quality factor accompanied by transmission zero realisation, wider upper stop-band with second harmonic suppression, and a considerable size reduction. The measured unloaded quality factor has been increased by a ratio of 60% in comparison to the conventional gap-coupled structures.

Introduction: Two basic direct and indirect coupling mechanisms are generally used for the design of microwave filters [1]. The discontinuities are employed to realise such couplings in the two main classes including aperture- and gap-coupled structures for 3D waveguide and planar structures, respectively [1, 2]. While gap-coupled discontinuity integrated with substrate-integrated waveguide (SIW) is reported as an alternative to decrease the size of the structure, operating at evanescent-mode [3], aperture-coupled discontinuity integrated with 3D resonators has been reported for high-quality and low-loss filter design [4]. Moreover, the aperture-coupled 3D cavity resonators solely realise transmission poles (TPs) above the 3D structure's cut-off frequency [5].

The realised TPs should be accompanied by transmission zeros (TZs) to demonstrate more selective filters. Several techniques have been reported to realise TZs in 3D waveguides or SIWs by integrating auxiliary sub-structures including bypassing couplings of non-resonating modes, side-wall cavities, and/or embedded metallic posts [5, 6]. Although the techniques are effective in TZs realisation, they all either add complexity in the design or increase the structure size. Recently, gap-coupled discontinuity has been studied to design 3D SIW band-pass filters (BPFs) for evanescent-mode TP realisation [2, 3].

Compared to the aperture-coupled excitation of 3D structures, the gap-coupled discontinuity demonstrates not only TP but also a TZ closed to the pass-band without any other auxiliary structure such as side-wall cavity or iris. However, this technique decreases the overall unloaded quality-factor (QF) of the resonator. In this Letter, a back-to-back integrated aperture- and gap-coupled discontinuity is proposed to design SIW BPFs. The developed structure is shown to take advantage of both discontinuities with an optimum performance including higher QF accompanied by TZ realisation, wider upper stop-band with second harmonic suppression, and a considerable size reduction.

Back-to-back aperture- and gap-coupled discontinuities: The integration of gap- and aperture-coupled discontinuities with SIW resonator is developed to accomplish size reduction and higher unloaded QF, respectively. In order to illustrate the superiority of the proposed concept, the frequency response of the gap-, aperture-coupled discontinuities, and their combination are separately discussed. Figs. 1*a–d* show the four designed structures to realise BPFs based on four types of discontinuities integrated with SIW, i.e. aperture-coupled, gap-coupled, a combination of aperture- and gap-coupled, and combination of aperture-coupled and two sides gap-coupled, respectively. EM-simulated S_{21}-parameters of the proposed structures are compared in Fig. 2. The SIW circuit integrated with multiple aperture-coupled (circuit (a)) realises a wide pass-band consisting of two TPs at around 4 and 5 GHz above the cut-off frequency, $f_c = 2.75$ GHz, with a maximum in-band insertion loss of 2.5 dB. However, its performance is restricted with a low upper-band suppression level, i.e. a maximum of 8.35 dB. The same platform is developed by implementing a gap-coupled discontinuity on the top wall of the SIW [3] instead of aperture one, as shown in Fig. 2*b*.

This configuration realises an evanescent-mode TP at 2.3 GHz along with two TZs at frequencies of 1.38 and 3.79 GHz. In comparison to the circuit (a), this structure is reported to demonstrate better performances in terms of lower 3 dB-fractional bandwidth (FBW), 9.13%, and TZs realisation, where the 20 dB spurious-free frequency range is limited to 0.96 GHz (2.9–3.86 GHz). Circuit (c) is obtained by integrating both circuits (a) and (b). The integrated structure realises a second-order pass-band at the centre frequency of 2.75 GHz with a 3 dB-FBW of 10.9% and a maximum in-band insertion loss of 2.93 dB.

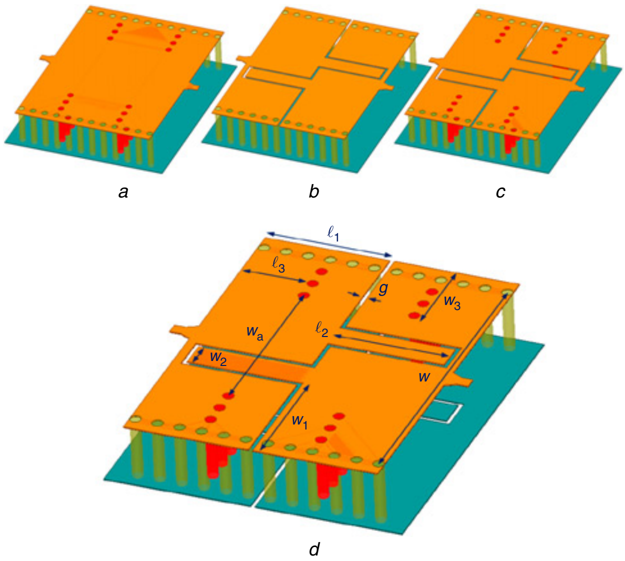

Fig. 1 *SIW BPFs based on*

a Aperture-coupled discontinuity
b Gap-coupled discontinuity
c Combination of gap- and aperture-coupled discontinuities
d Combination of aperture-coupled with two sides gap-coupled discontinuities

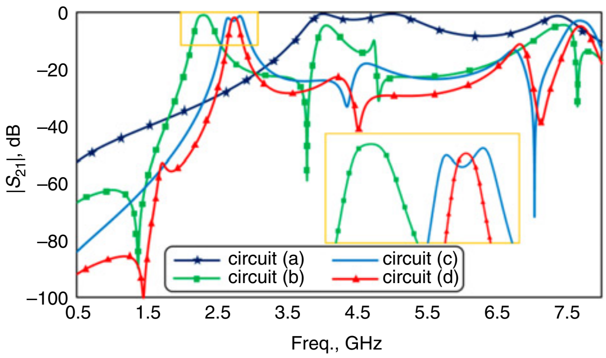

Fig. 2 *Full-wave simulated results of the structures in Fig. 1*

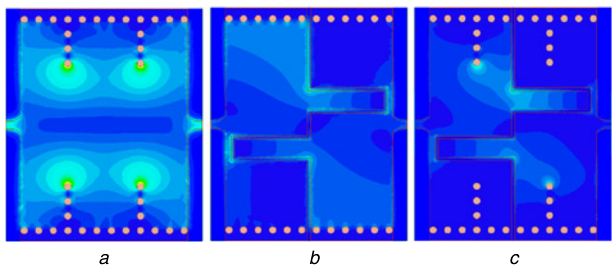

Fig. 3 *H-field distribution at resonance frequencies for*

a Circuit (a) at 4 GHz
b Circuit (b) at 2.3 GHz
c Circuit (d) at 2.75 GHz

Inspecting the simulated results, the unloaded QFs, using (1), are computed to be 104.7 and 47.7 for the circuits (b) and (c), respectively. Despite the new design in Fig. 1*c* extends the 20 dB spurious-free region to 1.29 GHz (3.23–4.52 GHz), its unloaded QF decreases by a ratio of 2.2 compared to that of the circuit (b). The circuit (c) can further be developed through duplicating the gap-coupled discontinuity to the ground wall of the SIW (see Fig. 1*d*). The proposed layout realises a first-order pass-band at 2.75 GHz with a 3 dB-FBW of 4.73% and a minimum in-band insertion loss of 1.81 dB. In comparison to the circuit (c), this structure is reported to demonstrate a narrower pass-band and a wider 20 dB spurious-free frequency range equal to 3.47 GHz (3.01–6.48 GHz). The unloaded QF is also found to be increased by a ratio of 2.36 as well. The simulated H-field distribution of circuits (a), (b), and (d) is depicted in Fig. 3 in which can be seen that the new structure (Fig. 3c) benefits both of the gap and aperture coupling mechanisms for electromagnetic waves filtering.

Size reduction compared to those of the cavity SIW BPFs and higher-quality factor than those of the gap-loaded SIW BPFs in the literature would be attributed to simultaneous involvement of the gap and aperture discontinuities, respectively. The insertion loss is given by

$$\mathrm{IL[dB]} = 10\mathrm{Log}\left(1 - Q_{\mathrm{L}}/Q_{\mathrm{un}}\right)^2 \quad (1)$$

where Q_{L} ($f_0/\Delta f_{3\mathrm{dB}}$) and Q_{un} stand for the loaded and unloaded QFs, respectively. The developed structure in Fig. 1d is fabricated on a single-layer 0.508 mm-thick Rogers RO4003 substrate (see Fig. 4) and tested by an Agilent 8722ES VNA. The simulated (Ansys HFSS) and measured S-parameters are compared in Fig. 5. A pass-band surrounded by two TZs at the central frequency of $f_0 = 2.74$ GHz is realised. As shown in Fig. 6, the pass-band can further be tuned at different central frequencies by varying the length of open-circuited stubs.

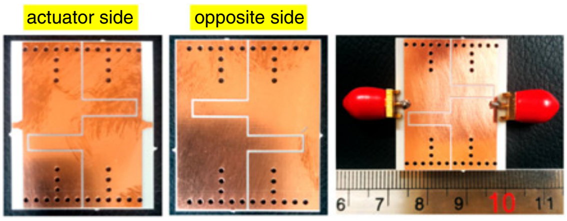

Fig. 4 *Digital photographs of the prototype SIW filter*

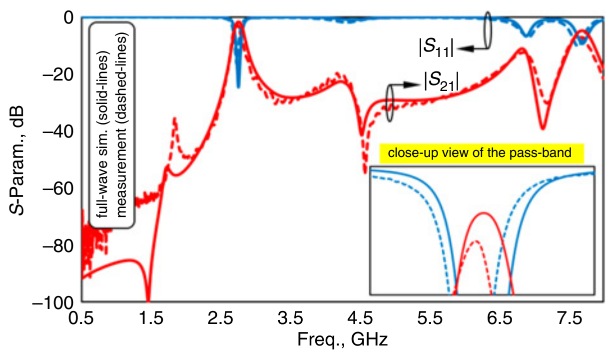

Fig. 5 *Measured and full-wave simulated results of the presented SIW BPF in Fig. 1d with the optimised values of $\ell_1 = 11.3$, $\ell_2 = 10.5$, $\ell_3 = 6$, $w = 29$, $w_a = 17$, $w_1 = 11.4$, $w_2 = 2.6$, $w_3 = 8$, and $g = 0.4$ (dimensions in mm). The diameter and centre-to-centre pitch of the via holes are 1 and 2 mm, respectively*

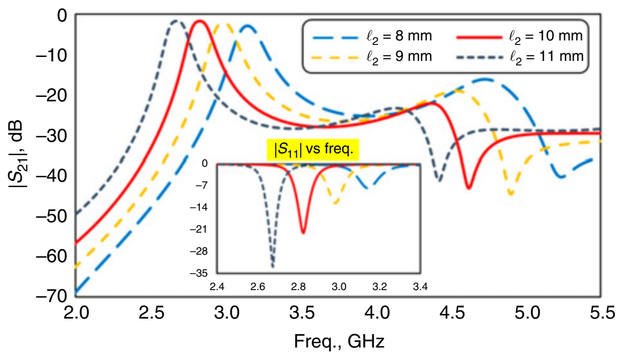

Fig. 6 *Controlling the pass-band and TZs frequencies by varying ℓ_2 parameter equal to 8 mm ($f_0 = 3.15$ GHz, IL = 2.9 dB, RL = 7.7 dB, and FBW = 4.44%), 9 mm ($f_0 = 2.99$ GHz, IL = 2.09 dB, RL = 12.5 dB, and FBW = 4.68%), 10 mm ($f_0 = 2.83$ GHz, IL = 1.71 dB, RL = 22 dB, and FBW = 4.59%), and 11 mm ($f_0 = 2.68$ GHz, IL = 1.69 dB, RL = 32.9 dB, and FBW = 4.85%). Inset shows the simulated return losses*

The measured insertion/return losses and 3 dB-FBW at the resonance frequency are reported to be around 2.5, 16.5, and 3.65%, respectively. The measured unloaded QF of the filter is around 109.5 versus that of 68.8 for the gap-coupled SIW in [3].

The occupied area excluding the coaxial-to-SIW transitions is 23 mm × 32 mm, i.e. $0.4\lambda_g \times 0.56\lambda_g$, where λ_g is the guided wavelength at the resonance frequency. The 20 dB spurious-free frequency range, as well as the ratio of the second spurious harmonic (f_s) to resonance frequency (f_0), are reported to be 3.47 GHz and 2.5, respectively. Table 1 summarises the performance of the developed back-to-back aperture- and gap-coupled BPF (new) compared to those of the recent SIW BPFs in the literature. The developed structure primarily offers a BPF with significant size reduction, higher QF, and wider upper stop-band.

Table 1: Proposed structure versus the conventional SIW BPF ones

Ref.	Filter order / technique	f_0, GHz	IL, dB	Q_{un}	f_s/f_0	Size ($\lambda_g \times \lambda_g$)
[3]	1st / gap	1.8	1.53	68.8	≃2	0.2 × 0.2
[7]	6th / cavity	5.5	1.7	46.9	≃1.45	1.34 × 0.69
[8]	4th / gap, cavity	33.03	1	91	(-)	1.33 × 3.21
[9]	5th / gap, cavity	8.5	1.1	20	≃2	0.68 × 1.36
New	1st / gap, cavity	2.74	2.5	109.5	2.5	0.4 × 0.56

Conclusion: A new class of back-to-back integrated aperture- and gap-coupled discontinuities has been developed to design SIW BPFs. The developed structure has been reported to take advantage of both discontinuities in the design of cavity and/or planar resonators with an optimum performance including higher QF accompanied by TZ realisation, wider upper stop-band with second harmonic suppression, and a considerable size reduction. The unloaded QF has been enhanced by a ratio of 60% in comparison to those of the gap-coupled SIW filters. Moreover, the ratio between the main and second harmonic has been increased by a factor of 2.5:1 compared to those of the conventional cavity SIW filters in the literature.

Submitted: *27 April 2020* E-first: *2 June 2020*
doi: 10.1049/el.2020.1221
One or more of the Figures in this Letter are available in colour online.

A. Nosrati and M. Mohammad-Taheri (*School of Electrical and Computer Engineering, University of Tehran, Tehran, Iran*)

✉ E-mail: mtaheri@ut.ac.ir

M. Nosrati (*National Research Council Canada/Conseil National de Recherches, Edmonton, AB, Canada*)

References

1 Matthaei, G.L., Young, L., and Jones, E.M.T.: ‘Microwave filters, impedance-matching networks, and coupling Structures’ (McGraw-Hill, New York, NY, USA, 1964)
2 Nosrati, M., and Daneshmand, M.: ‘Gap-coupled excitation for evanescent-mode substrate integrated waveguide filters’, *IEEE Trans. Microw. Theory Tech.*, 2018, **66**, (6), pp. 3028–3035
3 Nosrati, M., Abassi, Z., and Daneshmand, M.: ‘Single-layer capacitive excitation of substrate integrated waveguide evanescent-mode filter’, *IEEE Wirel. Microw. Compon. Lett.*, 2018, **28**, (12), pp. 1107–1109
4 Tomassoni, C., Silvestri, L., Ghiotto, A., *et al.*: ‘Substrate-integrated waveguide filters based on dual-mode air-filled resonant cavities’, *IEEE Trans. Microw. Theory Tech.*, 2018, **66**, (2), pp. 726–736
5 Amari, S., Rosenberg, U., and Bornemann, J.: ‘Singlets, cascaded singlets, and the nonresonating node model for advanced modular design of elliptic filters’, *IEEE Microw. Wirel. Compon. Lett.*, 2014, **14**, (5), pp. 237–239
6 Tomassoni, C., and Sorrentino, R.: ‘A new class of pseudoelliptic waveguide filters using dual-post resonators’, *IEEE Trans. Microw. Theory Tech.*, 2013, **61**, (6), pp. 2332–2339
7 Chu, P., Hong, W., Zheng, K.-L., *et al.*: ‘Balanced hybrid SIW–CPW bandpass filter’, *Electron. Lett.*, 2017, **53**, (25), pp. 1653–1655
8 Parment, F., Ghiotto, A., Vuong, T.-P., *et al.*: ‘Ka-band compact and high-performance bandpass filter based on multilayer air-filled SIW’, *Electron. Lett.*, 2017, **53**, (7), pp. 486–488
9 Chen, R.S., Wong, S.-W., Zhu, L., *et al.*: ‘Wideband bandpass filter using U-slotted substrate integrated waveguide (SIW) cavities’, *IEEE Microw. Wirel. Compon. Lett.*, 2015, **25**, (1), pp. 1–3